How to reduce the suspension thermal noise in LIGO without improving the Q's of the pendulum and violin modes.

V. B. Braginsky[1], Yu. Levin[2] and S. P. Vyatchanin[1]

[1] *Physics Faculty, Moscow State University, Moscow Russia*

[2] *Theoretical Astrophysics, California Institute of Technology, Pasadena, California 91125*

(February 7, 2008)

The suspension noise in interferometric gravitational wave detectors is caused by losses at the top and the bottom attachments of each suspension fiber. We use the Fluctuation-Dissipation theorem to argue that by careful positioning of the laser beam spot on the mirror face it is possible to reduce the contribution of the bottom attachment point to the suspension noise by several orders of magnitude. For example, for the initial and enhanced LIGO design parameters (i.e. mirror masses and sizes, and suspension fibers' lengths and diameters) we predict a reduction of ~ 100 in the "bottom" spectral density throughout the band $35 - 100$Hz of serious thermal noise.

We then propose a readout scheme which suppresses the suspension noise contribution of the top attachment point. The idea is to monitor an averaged horizontal displacement of the fiber of length l; this allows one to record the contribution of the top attachment point to the suspension noise, and later subtract it from the interferometer readout. This method will allow a suppression factor in spectral density of $7.4 \, (l/d^2) \, \sqrt{Mg/\pi E}$, where d is the fiber's diameter, E is it's Young modulus and M is the mass of the mirror. For the test mass parameters of the initial and enhanced LIGO designs this reduction factor is $132 \times (l/30\text{cm})(0.6\text{mm}/d)^2$.

We offer what we think might become a practical implementation of such a readout scheme. We propose to position a thin optical waveguide close to a fused silica fiber used as the suspension fiber. The waveguide itself is at the surface of a solid fused silica slab which is attached rigidly to the last mass of the seismic isolation stack (see Fig. 5). The thermal motion of the suspension fiber is recorded through the phaseshift of an optical wave passed through the waveguide. A laser power of 1mW should be sufficient to achieve the desired sensitivity.

I. INTRODUCTION

Random thermal motion will be the dominant noise source in the frequency band of $35 - 100$ Hz for the first interferometers [1] and in the frequency band of $25 - 126$ Hz for the enhanced interferometers [1] in the Laser Interferometer Gravitational Wave Observatory (LIGO) [2].

The thermal noise in this frequency band is caused by the losses in the suspension fibers, in particular at the top and the bottom of each fiber's attachment point. So far the only known way to reduce the thermal noise has been to improve the quality of the suspension fibers and their attachments. Here we suggest a different approach:

In Section II we will present a general analysis of the suspension noise based on a direct application of the Fluctuation-Dissipation theorem. We will explicitly separate the contributions to the thermal noise of the top and the bottom attachment points of the suspension fibers. It has been a common opinion that the top and bottom attachments contribute equally to the thermal noise. We shall challenge this point of view. In fact, we will show that if one shifts the laser beam spot down from the center of the mirror by an appropriately chosen distance h, the contribution of the bottom attachment point to the thermal noise can be reduced by several orders of magnitude. Fig. 3 presents plots of this reduction factor in the frequency band 35–100Hz for three different choices of h. What is plotted here is the ratio $S_{\text{bottom}}(f)/S_{\text{top}}(f)$, where $S_{\text{bottom}}(f)$ and $S_{\text{top}}(f)$ are the spectral densities of thermal noise contributed by the bottom and the top attachment points respectively. All three values of h are close to

---

[1] To be specific, we refer to the step 4 of LIGO enhancement — see [2]. In these the suspension thermal noise was calculated assuming the structural damping mechanism. However, the nature of dissipation in fused silica (e.g. viscous vs structural) is not yet fully established for the above frequency bands.

[2] The analysis of this paper is fully applicable to all other Interferometric Gravitational Wave detectors (e.g. VIRGO, GEO-600, TAMA etc.). For the sake of brevity in this paper we will refer only to LIGO.

$$h = \frac{I}{M(R+l)} \tag{1}$$

[cf. Eq(14)], where l is the length of the suspension fiber, I is the test-mass moment of inertia for rotation about the center of mass in the plane of Fig. 1 (see later), R is the radius of the mirror face and M is the mass of the test mass. The numerical values of these parameters for the initial and enhanced LIGO interferometers are

$$M = 10\text{kg}, \quad l = 30\text{cm}, \quad R = 12.5\text{cm}, \tag{2}$$

$$I = 4.73 \times 10^5 \text{g cm}^2, \quad h = 1.11\text{cm}.$$

Out of the three graphs presented in Fig. 3 the one with $h = 1.0$cm seems to be the optimal one. From the graphs we see that reduction factors of $\simeq 10^{-2}$ in the "bottom" component of the thermal noise is possible over the entire band of serious thermal noise: 35 to 100 Hz.

In Sec. IIIA we concentrate on the top attachment point. Lossy defects at the top create noise not only in the test mass motion, but also noise in the motion of the fiber. The latter is significantly larger than the former — by a factor of order $f^2/f_{\text{pendulum}}^2$ at frequencies above the pendulum frequency and below the violin resonances (which are the frequencies of interest for LIGO thermal noise). We show that if one monitors the average horizontal displacement of the suspension fiber of length l, one can essentially record the fluctuating "driving force" originating at the suspension top, and then subtract it from the interferometer's readout, thereby reducing thermal noise originating at the suspension top. The reduction factor in the spectral density of thermal noise is given by $P = 0.93 \cdot l/\lambda$ [cf. Eq(26)]. Here

$$\lambda = (d^2/8)\sqrt{\pi E/Mg} \tag{3}$$

is the length of the segment of fiber near it's top where the bending is greatest, d is the fiber's diameter, E is the fiber's Young modulus and g is the acceleration of gravity. For a fused silica fiber of diameter $d = 0.6$mm one gets a thermal noise reduction factor of $P \simeq 132$.

In Sec. IIIB we offer a particular way of implementing such a procedure. The basic idea is shown in Fig. 5. A fused silica slab is rigidly attached to the "ceiling" (i.e. to the last mass of the seismic isolation stack), and a waveguide ab is carved into the slab's surface. A monochromatic optical wave is set up in the waveguide, and a fused silica fiber used as the suspension fiber is positioned close to the waveguide, within the optical wave's evanescent field. When the fiber is displaced relative to the waveguide, it will change the optical wave's propagation speed, thus inducing an overall phaseshift of the wave. The detailed calculations in Sec. IIIB show that ~ 1mW of optical power in the wave is sufficient to reach the required sensitivity.

II. HOW TO REDUCE THERMAL NOISE ORIGINATING AT THE BOTTOM ATTACHMENT POINT

A. The model and formalism

The particular suspension that we consider is sketched in Fig. 1. We consider a compact rigid test mass of mass M suspended by a single fiber of length l and mass m; the fiber's bottom end is attached, for concreteness, to the top of the test mass (the main conclusions of this paper are also valid when the test mass is suspended by a fiber loop, as is planned for LIGO).

References [3], [4], [5], [7] give detailed explanations of how to use the Fluctuation-Dissipation theorem directly (without normal-mode decomposition) to calculate the spectral density of thermal noise [3]. In what follows we use the approach elaborated in [7].

To calculate the spectral density $S_x(f)$ of suspension's thermal noise at frequency f we imagine applying an oscillating force F perpendicular to the test mass's mirror surface at the center of the readout laser beam spot [4]:

---

[3]The original formulation of the Fluctuation-Dissipation theorem is given in [6]

[4]This prescription is only valid when the test masses are perfectly rigid, which is a good approximation when dealing with suspension thermal noise. The case when the test masses are no longer considered to be rigid (e.g. for an internal thermal noise calculations) is treated in detail in [7]. In that case the force $F(t)$ must be spread out over the laser beam spot instead of applied to it's center point.

$$F(t) = F_0 \cos(2\pi f t). \tag{4}$$

Then S_x is given by [cf. Eq (3) of [7]]

$$S_\mathrm{x}(f) = \frac{2k_\mathrm{B}T}{\pi^2 f^2} \frac{W_\mathrm{diss}}{F_0^2}, \tag{5}$$

where W_diss is the average power dissipated in the system (suspension, in our case) when the force $F(t)$ is applied, k_B is Boltzmann's constant and T is the temperature.

For concreteness, assume that the dissipation in the fiber occurs through structural damping (our conclusions will hold equally well for viscous or thermoelastic damping). In this case, the average power dissipated during the oscillatory motion of frequency f is given by [8]

$$W_\mathrm{diss} = 2\pi f U_\mathrm{max} \phi(f), \tag{6}$$

where U_max is the energy of the fiber's elastic deformation at a moment when it is maximally bent under the action of the oscillatory force in Eq. (4), and $\phi(f)$ is the "loss angle" of the material. The energy of the fiber's elastic deformation is given by

$$U = \frac{JE}{2} \int_0^l dz \, [y'']^2, \tag{7}$$

where E is the Young modulus of the fiber material, J is the geometric moment of inertia of the fiber (for a fiber with circular cross section of diameter d one has $J = \pi d^4/64$), z is distance along the fiber with $z = 0$ at the top and $z = l$ at the bottom, and $y(z)$ is the fiber's horizontal displacement from a vertical line.

This method of calculating thermal noise is useful for a qualitative analysis of the system, as well as quantitative analysis. In particular, it allows one to see which part of the suspension fiber contributes the most to the thermal noise. Assume, for a start, that the laser beam is positioned exactly in the middle of the mirror. Then to work out the thermal noise one has to imagine applying the oscillating force F in Eq. (3) to the mirror center; the motion of the fiber and the mirror under the action of the force are shown in Fig. 2a. Here we assume that the detection frequency f (and hence the frequency of the applied force) satisfies $f_p, f_r \ll f \ll f_v$, where f_p, f_r, f_v are the frequencies of the pendulum, rocking and first violin mode respectively (this condition implies that horizontal and rotational motion of the test mass is not affected by the presence of the fiber, and that the fiber itself remains straight).

From Fig. 2a it is clear that the fiber bends equally at the top and the bottom (we always assume that at the attachment point the fiber has to be normal to the surface to which it is attached). The total energy of elastic deformation is

$$U_0 = \frac{1}{2} Mg\lambda\alpha^2 = \frac{Mg\lambda}{2} \left(\frac{F}{M\omega^2 l} \right)^2, \tag{8}$$

where $\lambda = \sqrt{JE/Mg}$ is the characteristic length over which the fiber is bent near the attachment points, $\omega = 2\pi f$ is the angular frequency of detection, and α is the angle between the straight part of the fiber and the vertical.

The bending of the fiber at the bottom can be avoided if one applies the force F in Eq. (4) not at the middle of the mirror, but at some distance h below the center. In particular, we should choose h so that the mirror itself rotates by the same angle as the fiber under the action of the applied force; the resulting motion is shown on Fig. 2b. Physically this means that if we position our laser beam at a distance h below the mirror center, then the bottom attachment point will not contribute to the thermal noise when h is carefully chosen. This means that the overall suspension noise will be reduced by a factor of order 2 (in fact, more precisely, by a factor of $2(1 + R/l)$, where R is the radius of the mirror and l is the length of the string, — see later in this section).

In the rest of this section and Appendix A we find the general expression for the suspension thermal noise, and we then work out the optimal h for the frequency band of interest for LIGO. We will assume that when a periodic oscillation of frequency f is induced in the system, the average power dissipated as heat in the suspension is given by

$$W_\mathrm{diss} = f \left[\zeta_\mathrm{top}(f)\bar{\alpha}_\mathrm{T}^2 + \zeta_\mathrm{bottom}(f)\bar{\alpha}_\mathrm{B}^2 \right]. \tag{9}$$

Here $\bar{\alpha}_\mathrm{T}$ and $\bar{\alpha}_\mathrm{B}$ are the amplitudes of oscillations of the angles α_T and α_B respectively (see Fig. 1), and ζ_top and ζ_bottom are frequency-dependent quantities characterizing dissipation at the top and the bottom respectively. For the case of structural damping

$$\zeta_\mathrm{top} = \zeta_\mathrm{bottom} = \pi f \phi(f) Mg\lambda, \tag{10}$$

where λ is given by Eq. (3) of the introduction.

To compute W_{diss} we need to evaluate $\bar{\alpha}_{\text{T}}$ and $\bar{\alpha}_{\text{B}}$ by analyzing the dynamics of the oscillations. This is done in Appendix A, see Eqs. (40) and (39). Putting these equations into Eq. (9) and then into Eq. (5), we obtain [cf. Eq. (41)]

$$S_{\text{x}}(f) = \frac{4k_{\text{B}}T}{\pi\omega} \left\{ \frac{I/M - R(g/\omega^2 + h)}{[Ig - MgR(g/\omega^2 - R)]\cos(kl) - (I\omega^2 - MgR)\sin(kl)/k} \right\}^2$$
$$\times \left\{ \zeta_{\text{top}} + \zeta_{\text{bottom}} \cos^2(kl) \left[\frac{I/M - h\left[R + \tan(kl)/k - g/\omega^2\right]}{I/M - R(g/\omega^2 + h)} \right]^2 \right\}. \tag{11}$$

Here $k = \omega/c = 2\pi f/c$, $c = \sqrt{glM/m}$ is the speed of propagation of a transverse wave in the fiber. From the above equation we can infer the ratio of the bottom and the top contributions to the thermal noise:

$$\frac{S_{\text{bottom}}(f)}{S_{\text{top}}(f)} = \frac{\zeta_{\text{bottom}}(f)}{\zeta_{\text{top}}(f)} \cos^2(kl) \left[\frac{I/M - h\left[R + \tan(kl)/k - g/\omega^2\right]}{I/M - R(g/\omega^2 + h)} \right]^2. \tag{12}$$

This is the most important equation in this section of the paper; it will be discussed in the next subsection.

B. The case of low-frequency suspension noise

When the detection frequency f is far below the frequency of the fundamental violin mode, f_{v}, then $kl \ll 1$ in Eq. (12) and

$$\frac{\tan(kl)}{k} \simeq l\left[1 + \frac{1}{3}(kl)^2\right]. \tag{13}$$

Let us assume that the top and the bottom are equally lossy, i.e. $\zeta_{\text{top}} = \zeta_{\text{bottom}}$, as the would be for structural damping, Eq (10) above. We choose h to be

$$h = \frac{I}{M(R+l)}. \tag{14}$$

Putting Eqs (14) and (13) into Eq. (12), we get

$$\frac{S_{\text{bottom}}(f)}{S_{\text{top}}(f)} \simeq \frac{\pi^4}{9} \frac{1}{\left[1 - (R/h)(\omega_p^2/\omega^2)\right]^2} \left(\frac{f}{f_{\text{v}}}\right)^4, \tag{15}$$

where $\omega_p = \sqrt{g/l}$.

For the initial and enhanced LIGO design $f_{\text{v}} \simeq 400\text{Hz}$, $M \simeq 10\text{kg}$, $I \simeq 4.73 \times 10^{-2}\text{kg} \times \text{m}^2$, $R \simeq 12.5\text{cm}$, and the interesting frequency range where suspension noise is expected to dominate is $35 - 100\text{Hz}$ (actually, this depends on the stage of enhancement. The frequency band specified above is where the suspension thermal noise is expected to dominate in the initial LIGO; in the enhanced version this frequency interval will be larger). In this case Eq. (15) gives $S_{\text{bottom}}(f)/S_{\text{top}}(f) \simeq 0.002 - 0.2$.

In Fig.3 we give plots for $S_{\text{bottom}}/S_{\text{top}}$ as a function of the detection frequency f for three different choices of h. We have used Eq. (15) to make all the plots and we set I, M, R and l to the numerical values appropriate for the initial and enhanced LIGO design and given at the beginning of this section.

The first curve is plotted for h given by Eq. (14), in our case $h = 1.11\text{cm}$. The second and third curves are for $h = 1.0\text{cm}$ and $h = 0.9\text{cm}$; these values of h are chosen so that $S_{\text{bottom}}/S_{\text{top}} = 0$ for $f = 80\text{Hz}$ and $f = 105\text{Hz}$ respectively. Out of the three cases the choice $h = 1\text{cm}$ gives the best overall performance across the considered frequency band, with the typical reduction factor of

$$\frac{S_{\text{bottom}}}{S_{\text{top}}} \sim 10^{-2}. \tag{16}$$

¿From Eq. (11) we see that choosing h close to the value in Eq. (14) reduces the total suspension thermal noise by a factor close to $2(1 + R/l) \sim 3$ relative to the case when $h = 0$.

C. High-frequency suspension thermal noise

A somewhat less interesting observation is that for $h = 0$ and $f_{\mathrm{n}} = f_{\mathrm{v}}(n + 1/2)$, where n is an integer,

$$\frac{S_{\mathrm{bottom}}(f_{\mathrm{n}})}{S_{\mathrm{top}}(f_{\mathrm{n}})} = 0. \tag{17}$$

Unfortunately, at $f = f_{\mathrm{n}}$ the interferometer's noise is dominated by shot noise. However, if one uses an advanced optical topology — for example, resonant sideband extraction — then it is possible to reduce the shot noise in a narrow band around any chosen frequency. Then the thermal noise may dominate in this narrow band, and our observation (17) may be useful in case one tries to reduce the thermal noise by cooling of the fiber top.

III. HOW TO CONTROL NOISE FROM THE TOP

A. The concept

In this section we propose a recipe for how to decrease the influence of the thermally fluctuating stress at the top part of the suspension fiber. The basic idea is the following:

Intuitively, the fluctuations at the top cause bending of the fiber at the top, which will be a random process in time. This random bending will randomly move the rest of the fiber and ultimately drive the random motion of the test mass. We propose to measure directly the thermally driven fluctuations in the horizontal displacement of the fiber, and from them infer the fluctuating force which drives the random motion of the mirror. We can then subtract the motion due to this fluctuating force from the interferometer output[5].

Formally this amounts to introducing a new readout variable q as follows:

$$q = X_{\mathrm{mirror}} + X_{\mathrm{fiber}}. \tag{18}$$

Here X_{mirror} is the horizontal displacement of the laser spot's center (i.e.the signal ultimately read by the interferometer's photodiode), and

$$X_{\mathrm{fiber}} = \int_0^l dz \Phi(z) y(z) \tag{19}$$

is the fiber's horizontal displacement weighted by some function $\Phi(z)$ to be discussed below. We will postpone the discussion of how to measure q experimentally until the next section; here we concentrate on finding the optimal $\Phi(z)$ and seeing what is the maximal possible reduction in the thermal noise.

To find the spectral density of fluctuations in q we need to imagine acting on the system with sinusoidal force $F_q \propto \cos(2\pi f t)$ that appears in the interaction hamiltonian in the following way

$$H_{\mathrm{int}} = -q F_q = -X_{\mathrm{mirror}} F_q - \int_0^l dz F_q \Phi(z) y(z); \tag{20}$$

cf. the discussion of the Fluctuation-Dissipation theorem in Ref. [7]. From the Eq. (20) we observe that applying the generalized force F_q to the system is equivalent to applying two forces simultaneously: one is a force of magnitude F_q applied to the mirror surface at the center of the beam spot, and the other is a force distributed along the fiber in the following manner:

$$\frac{dF_{\mathrm{fiber}}}{dz} = F_q \Phi(z). \tag{21}$$

The resulting motion of the system is shown in Fig. 4. The intuitive idea is to choose the weighting function $\Phi(z)$ so that when the beam spot's height h has also been appropriately chosen, F_q induces no bending of the fiber at the top or at the bottom.

---

[5]The idea of thermal noise compensation is not new (e.g. [11], [10]). However, our detailed treatment and concrete experimental proposal is different from anything prior to this paper.

In the case of structural damping the dissipated power is proportional to the elastic energy U of the fiber. Thus formally one has to choose $\Phi(z)$ and h so that U is minimized. It is convenient to reformulate the problem: to find the shape of the fiber $y(z)$ and beam-spot height h for which the functional in Eq. (7) has a minimum, and after this calculate the distribution $\Phi(z)$ of the driving force on the fiber that will produce the desired shape $y(z)$. In Appendix B we carry out this straightforward but somewhat tedious task. We obtain [cf. Eq. (50)]

$$y_{\text{optimal}}(z) = \frac{F_q}{M\omega^2}\left(\frac{z}{l}\right)^2\left(\frac{3(r+1)-z/l}{2(3r^2+3r+1)}\right)$$
$$\simeq \frac{F_q}{M\omega^2}\left(\frac{z}{l}\right)^2\left(0.76 - 0.18\frac{z}{l}\right). \tag{22}$$

Here $r = R/l$, R is the radius of the mirror, l is the length of the fiber, $\omega = 2\pi f$ is the angular frequency of detection. We substitute here and below $r = 0.42$ corresponding to the initial and enhanced LIGO test masses. The profile of the distributed force acting on the fiber and hence of $\Phi(z)$ is mainly determined by $y''(z)$ (see Appendix B):

$$\Phi(z) \simeq \Phi_0 = -\frac{Mg}{F_q}y''(z), \tag{23}$$

which gives [cf. Eq. (53)]

$$\Phi_0(z) \simeq -\frac{\omega_p^2}{\omega^2 l}\left(1 + r - \frac{z}{l}\right)\frac{3}{3r^2+3r+1}$$
$$= -\frac{\omega_p^2}{\omega^2 l}\left(1.53 - 1.08\frac{z}{l}\right), \tag{24}$$

where $\omega_p = \sqrt{g/l}$. When the force distribution has this optimal form, the elastic energy has the minimum value

$$U_{\min} \simeq \frac{3}{3r^2+3r+1}\frac{\lambda}{l}\frac{Mg\lambda}{2}\left(\frac{F_q}{M\omega^2 l}\right)^2$$
$$= \frac{1.08\lambda}{l} \times U_0, \tag{25}$$

where U_0 is the elastic energy in Eq. (8). Therefore, for a fused silica fiber with $E \simeq 6.9 \times 10^{10}$Pa and $d = 0.6$mm, we get $\lambda \simeq 2.1$mm and the maximal reduction factor for the spectral density of suspension thermal noise is

$$P = \frac{l}{1.08\lambda} \simeq 132. \tag{26}$$

B. Experimental realization–a proposal

1. Preliminary remarks

Before describing a particular experimental realization of the above scheme, a few general remarks are in order.

First, one might worry that our averaging function $\Phi(z)$ is frequency dependent — in general, that could make the experimental implementation very difficult. In particular [see Appendix B, Eq.(52)], Φ consists of two components: $\Phi = \Phi_0 + \Phi_1$, where Φ_0 and Φ_1 as given by Eq. (52) have very different frequency dependence. However at the frequencies of interest $\Phi_0 \gg \Phi_1$, and then the approximate formula (24) for the averaging function $\Phi(z) = \Phi_0(z)$ is a product of two terms: one which depends only on the frequency f (i.e. $\Phi(z) \propto 1/f^2$), and the other which depends only on the coordinate z. This feature makes the scheme feasible for a broad range of frequencies. It is sufficient that our device measures the displacement of the fiber with the frequency-independent averaging function $\tilde{\Phi}(z) \propto f^2 \times \Phi(z)$, and that the frequency dependence is then put back in during data analysis when constructing the readout variable q:

$$q = X_{\text{mirror}} + \eta(f)\int_0^l dz\tilde{\Phi}(z)y(z), \tag{27}$$

where $\eta(f) \propto f^{-2}$ is chosen so that $\eta\tilde{\Phi} = \Phi$.

As mentioned above, Eq. (24) is an approximation valid when the fiber has no inertia, i.e. when $f \ll f_v =$ (lowest violin-mode frequency). When the inertia of the fiber becomes important ($\Phi_1 \sim \Phi_0$), it is no longer possible to factor out a frequency-dependent part of Φ. As a result, when f gets closer to f_v, the effectiveness of the thermal noise suppression (i.e. the value of P) is reduced. A detailed analysis shows that if we choose $\tilde{\Phi}(z)$ so that the thermal noise compensation is optimal ($P = P_{\max}$) at low frequencies $f \ll f_v$, then at $f = 0.2f_v$ we have $P \sim 0.9P_{\max}$, at $f = 0.32f_v$ we have $P \sim 0.5P_{\max}$, and beyond this P is reduced sharply as we approach the first violin mode. For the fused silica fiber discussed above $f_v \sim 400\text{Hz}$, so the compensation is effective throughout the band $35 - 100\text{Hz}$ where suspension thermal noise dominates. It is worth emphasizing that this deterioration in the reduction factor only happens when we use the averaging function Φ_0 instead of $\Phi_0 + \Phi_1$ close to the violin frequency. Thus, this limitation is one of technology and not of principle. Perhaps, it is possible to conceive of a scheme where the correct averaging function is implemented at all frequencies. However, we have not been able to do so.

Secondly, any sensor used for monitoring the fiber coordinate X_{fiber} will have an intrinsic noise which will deteriorate the quality of the thermal-noise compensation. In particular, the overall reduction factor P_{eff} is given by

$$\frac{1}{P_{\text{eff}}} = \frac{1}{P} + \frac{S_{\text{fiber meas}}(f)}{S_{\text{fiber therm}}(f)}, \tag{28}$$

where $S_{\text{fiber meas}}(f)$ is the spectral density of intrinsic noise of the device which measures the average displacement of the fiber and $S_{\text{fiber therm}}(f)$ is the spectral density of thermal fluctuations of the same displacement.

For the case of structural damping it is easy to estimate

$$\sqrt{S_{X \text{ fiber therm}}(f)f} \sim \sqrt{\frac{\lambda \phi kT}{Mg}} \sim 10^{-14}\text{cm}, \tag{29}$$

where we assume that $\phi \sim 10^{-7}$ for fused silica. If our goal is to achieve $P \sim 100$ then the condition $P_{\text{eff}} \simeq P$ implies

$$\sqrt{S_{\text{fiber meas}}f} << \sqrt{\frac{S_{\text{fiber therm}}f}{P}} \sim 10^{-15}\text{cm}. \tag{30}$$

We shall take the above number as a sensitivity goal that our measuring device should achieve.

2. Proposed measuring device

Now we are ready to describe a possible practical implementation of our thermal-noise compensation scheme. Figure 5 illustrates the basic idea. We propose to use a fused silica optical fiber with the refractive index n_1 for the test mass's suspension. Next to this fiber we attach to the top seismic isolation plate (i.e. the "ceiling") a rigid block of the fused silica A with the same index of refraction n_1. On the surface of this rigid block we put a thin optical waveguide with refractive index n_2 such that $n_2 > n_1$, so that the waveguide is at a distance $\sim \lambda_{\text{optical}}/2\pi$ from the suspension fiber. It is assumed that the side of the waveguide close to the suspension fiber does not have any coating, i.e. it is "naked". In this configuration the optical wave may propagate through the waveguide without substantial scattering even though the suspension fiber is within the wave's evanescent zone. This device will produce a relatively large response to the displacement X_{fiber} in the form of a phaseshift of $\Delta\phi$ of the optical wave:

$$\Delta\phi = K\frac{2\pi X_{\text{fiber}}}{\lambda_{\text{optical}}}\frac{2\pi l}{\lambda_{\text{optical}}}, \tag{31}$$

where the dimensionless factor K depends on the values of n_1 and n_2 and for typical optical waveguides is $K \sim 10^{-3}$. Equation (31) implies that in order to register $X_{\text{fiber}} \sim 10^{-15}\text{cm}$ we need a sensitivity $\Delta\phi \sim 10^{-7}$. Thus for averaging time of $\tau_{\text{grav}} = 0.01\text{sec}$ we need to use the power of coherent light of $W \sim 1\text{mW}$. This power can be decreased if one uses a resonant standing wave in the waveguide.

Apart from the shot noise of the laser light, let us briefly discuss two other kinds of noise in this sensor. A more complete discussion will be presented elsewhere.

The first kind is seismic noise. A simple calculation shows that the seismic contribution to the noise in the readout variable q is about twice as large in spectral density as the seismic contribution to the noise in X_{mirror}. Thus the seismic noise will not be an issue at frequencies above the "seismic wall" of the LIGO sensitivity curve.

The second kind of noise we want to mention is the mechanical thermal fluctuations of the waveguide itself. Our estimates show that if these fluctuations are caused by structural damping (and not by some surface or contact defects), then the ratio of the mechanical thermal fluctuations of the waveguide to those of the fiber is

$$\frac{S_{\text{waveguide}}}{S_{\text{fiber}}} \sim \frac{Mg}{El\lambda} \sim 10^{-5}. \tag{32}$$

Thus, if the system is sufficiently clean then the mechanical thermal fluctuations of the waveguide will probably not significantly reduce the sensitivity of our sensor.

It is worth noting that in order to achieve the optimal compensation of thermal noise, the distance $d(z)$ between the suspension fiber and the waveguide has to vary in accord with the optimal profile of the averaging function:

$$d = A - B \log [\Phi(z)], \tag{33}$$

where A and B are constants to be discussed elsewhere. In this case the phase of the waveguide's output records the optimally averaged coordinate X_{fiber} of the fiber.

The profile $d(z)$ may be difficult for experimental realization. However we find that in the simplest case when $\Phi(z)$ is a constant over the length l of averaging, the factor P is reduced very little: from $P = 132$ to $P \sim 120$.

IV. CONCLUSION

In this paper we have done two things.

Firstly, we have shown that by an appropriate positioning of the laser's beam spot on the surface of each test-mass mirror, one can reduce the contribution of the suspension fiber's bottom to the suspension thermal noise by two to three orders of magnitude in the frequency band of $35 - 100$Hz for the initial LIGO design.

Secondly, we have proposed a way to compensate the suspension thermal noise originating from the top of each fiber by monitoring independently the fiber's random horizontal displacement. In the best case, with the system parameters for the initial or enhanced LIGO design, one can get a reduction factor of the order of $P = 130$ in spectral density over the entire $35 - 100$Hz band, when both the first and second procedures are applied; and with realistic defects in the design one should be able to get a reduction of at least $P \simeq 100$

The device that compensates the suspension thermal noise can ease the requirements to quality of suspension system. In particular, if this device allows the reduction factor of $P = 100$, this would effectively increase the quality factors of pendulum and violin modes by a factor of $P = 100$. So far the highest quality factor $Q \simeq 10^8$ of the pendulum mode was achieved in [9] for a fused silica suspension fiber, which allows one to reach the Standard Quantum Limit for averaging time of 10^{-3}sec. Implementation of our proposal could effectively increase this quality factor to $Q_{\text{eff}} \simeq 10^{10}$, which would reduce the thermal noise in LIGO to the level of Standard Quantum Limit for averaging time of 10^{-2}sec. Then the techniques which allow one to beat the Standard Quantum Limit (see e.g. [13]) could be used in the enhanced LIGO interferometers.

ACKNOWLEDGMENTS

APPENDIX A

In this appendix we solve the dynamical problem of finding the amplitudes $\bar{\alpha}_{\text{T}}$ and $\bar{\alpha}_{\text{B}}$ of oscillation of the top and bottom bending angles in Eq. (9) when a periodic force

$$F = F_0 \cos(\omega t) \tag{34}$$

is applied to the mirror at a distance h below the mirror center [we use these amplitudes in Eq. (9) of the text]. For convenience we complexify all of the quantities:

$$F = F_0 e^{\imath \omega t}, \quad \alpha_{\text{T}} = \bar{\alpha}_{\text{T}} e^{\imath \omega t}, \quad \alpha_{\text{B}} = \bar{\alpha}_{\text{B}} e^{\imath \omega t},$$

$$x = \bar{x} e^{\imath \omega t}, \quad \psi = \bar{\psi} e^{\imath \omega t},$$

where x is the displacement of the test mass's center of mass and ψ is the angle by which the mirror is rotated (see Fig. 1) under the action of the force $F(t)$. As usual, $\omega = 2\pi f$ is the angular frequency.

¿From the projection of the Newton's Second Law on the horizontal axis we have

$$F_0 - (\bar{\alpha}_B - \bar{\psi})Mg = -M\omega^2\bar{x}, \tag{35}$$

and, for the rotational degree of freedom, the equation of motion is

$$F_0 h + MgR\bar{\alpha}_B = I\omega^2\bar{\psi}, \tag{36}$$

where R is the radius of the test-mass cylinder and I is the moment of inertia for rotation about the test-mass center of mass in the plane of the Fig. 1. In the two equations above we assume that α_B and ψ are small.

The fiber's horizontal displacement y from a vertical line approximately satisfies the wave equation:

$$\frac{\partial^2 y}{\partial t^2} = c^2 \frac{\partial^2 y}{\partial z^2}, \tag{37}$$

where z is distance along the wire, with $z = 0$ at the top and $z = l$ at the bottom, and $c = \sqrt{glM/m}$ is the transverse speed of sound in the wire. In this Appendix we use Eq. (37) for flexible wire since it's solutions are simple. If one takes the stiffness into account this changes the solutions of Eq. (37) by a relative order of λ/l, see e.g. [12]. However, when using Eq. (37), we must allow non-zero bending angles at the top and bottom attachment points, α_T and α_B. The energy of elastic strain of the wire then consists of two components: one from the bulk of the wire given by Eq. (7), and the other from the bending at the attachment points given by Eq. (8). The solution to Eq. (37) is

$$y(z,t) = A\sin(kz)\,e^{\imath\omega t}, \tag{38}$$

where $k = \omega/c$ is the wave vector of an off-resonance standing wave induced in the fiber and A is a constant. The boundary condition is set at the bottom by

$$A\sin(kl) = \bar{x} + R\bar{\psi}$$
$$kA\cos(kl) = (\bar{\alpha}_B - \bar{\psi}).$$

Putting these two equations into Eqs. (35) and (36), we find

$$\bar{\alpha}_B = -F_0 \frac{I/M - h\left[R + \tan(kl)/k - g/\omega^2\right]}{MgR^2 + (I\omega^2 - MgR)\left[g/\omega^2 - \tan(kl)/k\right]} \tag{39}$$

and

$$\bar{\alpha}_T = -F_0 \frac{I/M - R(g/\omega^2 + h)}{[Ig - MgR(g/\omega^2 - R)]\cos(kl) - (I\omega^2 - MgR)\sin(kl)/k}. \tag{40}$$

Putting Eqs. (39), (40) and (9) into Eq. (5), we finally get for the spectral density of the suspension thermal noise:

$$S_x(f) = \frac{4k_B T}{\pi\omega}\left\{\frac{I/M - R(g/\omega^2 + h)}{[Ig - MgR(g/\omega^2 - R)]\cos(kl) - (I\omega^2 - MgR)\sin(kl)/k}\right\}^2$$
$$\left\{\zeta_{\text{top}} + \zeta_{\text{bottom}}\cos^2(kl)\left[\frac{I/M - h\left[R + \tan(kl)/k - g/\omega^2\right]}{I/M - R(g/\omega^2 + h)}\right]^2\right\}. \tag{41}$$

APPENDIX B

Here we calculate the optimal shape $y_{\text{optimal}}(z)$ of the fiber and the vertical position of the laser beam spot h that minimize the fiber's elastic deformation energy [Eq. (7)].

It is easy to deduce from Eq. (7) that energy minimizing function $y(z)$ obeys the equation $y''''(z) = 0$. Therefore

$$\frac{y(z)}{l} = a_0 + a_1\frac{z}{l} + a_2\frac{z^2}{l^2} + a_3\frac{z^3}{l^3}, \tag{42}$$

9

where a_i are constants to be determined.

Let us discuss the boundary conditions. Strictly speaking, the boundary conditions should be such that the fiber is perpendicular to the surface of attachment at both the top and the bottom. Therefore at the top we have $y(0) = y'(0) = 0$, from which immediately follows $a_0 = a_1 = 0$. However, at the bottom it is more convenient for our calculations embody the bending of the fiber, on the lengthscale λ, in a bending angle α_B as in Fig. 1, and correspondingly add an additional term

$$U_{\text{add}} = (1/4)Mg\lambda\alpha_B^2 \tag{43}$$

to the energy functional in Eq. (7), and then in Eq. (42) evaluate $y(l)$ and it's derivatives above the λ-scale bend. Our energy minimization procedure will make the angle α_B so small that the additional elastic energy as given by Eq. (43) is negligible compared to U in Eq. (7)

The coefficients a_2 and a_3 can be inferred from force and torque balance at the test mass:

$$F_q - Mgy'(l) = -M\omega^2(y(l) + R(y'(l) + \alpha_B)), \tag{44}$$

and

$$F_q h - MgR\alpha_B = -I\omega^2(y'(l) + \alpha_B).$$

It is useful to rewrite these equations in a dimensionless form:

$$\xi(1 + \eta(r - a)) + r\alpha_B = -\xi_0,$$
$$\eta\xi + \alpha_B(1 - \mu ra) = -\mu s\xi_0; \tag{45}$$

where

$$\xi = \frac{y(l)}{l}, \quad \eta = \frac{y'(l)l}{y(l)}, \quad s = \frac{h}{l},$$

$$a = \frac{\omega_p^2}{\omega^2} \simeq 10^{-3} \div 10^{-6}, \quad r = 0.42, \quad \mu = \frac{Ml^2}{I} = 19,$$

where $\omega_p = \sqrt{g/l}$. Here we have used for estimates the mirror parameters for the initial and enhanced LIGO interferometers. Solving the above system of equations (45) for ξ and α_B (taking η as a parameter) we get:

$$\alpha_B = \xi_0 \frac{\eta - \mu s(1 + \eta(r - a))}{[1 + \eta(r - a)][1 - \mu ra] - r\eta} \simeq \xi_0[\eta - \mu s(1 + \eta(r - a))]$$

$$\xi = -\xi_0 \frac{1 - \mu r(a + s)}{[1 + \eta(r - a)][1 - \mu ra] - r\eta} \simeq -\xi_0(1 - \mu r(a + s))$$

Let us choose the parameter s so that $\alpha_B = 0$ for some angular frequency ω_0 in the frequency band $35 - 100$Hz where thermal noise is most serious:

$$s \simeq \frac{\eta}{\mu[1 + \eta(r - a_0)]} \simeq \frac{\eta}{\mu[1 + \eta r]}, \quad a_0 = \frac{\omega_p^2}{\omega_0^2} \tag{46}$$

Then we get for α_B and ξ

$$\alpha_B \simeq \xi_0 \frac{\eta^2}{1 + \eta r}(a - a_0) \tag{47}$$

$$\xi \simeq -\xi_0 \frac{1}{1 + \eta r}.$$

We can express the coefficients a_3 and a_2 in terms of ξ and η by combining Eqs. (42) and (45), and we can then calculate the elastic energy according to Eq. (7):

$$U \simeq \frac{Mg\lambda}{2} \left(\frac{F_q}{M\omega^2 l} \right)^2 \times \frac{\lambda}{l} \times \frac{4(\eta^2 - 3\eta + 3)}{(1 + r\eta)^2} \tag{48}$$

This function has the minimal value

$$U_{\text{min}} \simeq \frac{l}{\lambda} \times \frac{3}{1 + 3r + 3r^2} \times U_0 = \frac{1.08\lambda}{l} \times U_0$$

at optimal η given by

$$\eta_{\text{opt}} = \frac{3(1 + 2r)}{2 + 3r} = 1.69. \tag{49}$$

Here U_0 is the energy of elastic strain of the fiber when the force of magnitude F_q is applied in mirror center, as worked out in Eq. (8). Now we can figure out the optimal shape of the fiber's horizontal displacement:

$$y_{\text{optimal}}(z) = \frac{F_q}{M\omega^2} \left(\frac{z}{l} \right)^2 \left(\frac{3(r + 1) - z/l}{2(3r^2 + 3r + 1)} \right)$$
$$\simeq \frac{F_q}{M\omega^2} \left(\frac{z}{l} \right)^2 \left(0.76 - 0.18\frac{z}{l} \right). \tag{50}$$

From Eq. (46) we get $h = l \times s \simeq 1.55$cm.

Using (47) one can show that $\alpha_{\text{B}} \leq 1.7 \cdot 10^{-3} \cdot \xi_0$ over the frequency band $35 - 100$Hz. From this and Eq. (43), one can compute the energy due to the bending at the fiber bottom: $U_{\text{add}} \simeq 1.4 \cdot 10^{-6} \times E_0$. We see that $U_{\text{add}} \ll U_{\text{min}}$ and hence over the frequency band of interest the small bending at the bottom does not contribute significantly to the total energy of elastic deformation.

The profile of the distributed force and correspondingly the function Φ are given by

$$F_q\Phi(z) = -\rho\omega^2 y(z) - Mgy''(z) + IEy''''(z). \tag{51}$$

Here ρ is the fiber density per unit length. Since $y''''(z) = 0$, the function Φ consists of two terms $\Phi(z) = \Phi_0(z) + \Phi_1(z)$, where

$$\Phi_0(z) = -\frac{Mg}{F_q}y''(z), \quad \Phi_1(z) = -\frac{\rho\omega^2}{F_q}y(z). \tag{52}$$

$$\Phi_0(z) = \frac{\omega_p^2}{l\omega^2} \cdot \left(1 + r - \frac{z}{l} \right) \cdot \frac{3}{3r^2 + 3r + 1} = \frac{\omega_p^2}{l\omega^2} \cdot \left(1.53 - 1.08\frac{z}{l} \right). \tag{53}$$

We see that Φ_0 is much greater than Φ_1 in our frequency range ($10 - 100$Hz for the initial LIGO).

---

[1] A. Abramovici *et. al.*, Science, **256**, 325 (1992); C. Baradaschia *et. al.*, Nucl. Instrum & Methods, **A289**, 518 (1990).

[2] B. Barish *et. al.*, "LIGO advanced Research and Development Program Proposal", LIGO technical document LIGO-M970107-00-M (Caltech, 1996).

[3] G. I. Gonzalez and P. R. Saulson, *J. Accoust. Soc. Am*, **96**, 207-212 (1994).

[4] N. Nakagawa *et. al.*, *Rev. Sci. Instrum.* **68(9)**, 1-4 (1997).

[5] A. V. Gusev *et. al.*, *Radiotekhnika i Elektronika*, **40**, 1353-1359 (1995).

[6] H. B. Callen and T. A. Welton, *Phys. Rev.* **83**, 3 4-50 (1951).

[7] Yu. Levin, *Phys. Rev. D*, **57**, 659-663 (1998) .

[8] P. R. Saulson, *Phys. Rev. D*, **42**, 2437-2445 (1990).

[9] V. B. Braginsky, V. P. Mitrofanov, K. V. Tokmakov, *Phys. Lett. A*, **218**, 164-166 (1996) and references therein.

[10] V. V. Kulagin, First E. Amaldi conference on grav. wave experiments, editors E.Coccia, G.Pizzella, F.Ronga, World Sci. Publ. Comp., 1995, p. 328..

[11] Remarks by R. Weiss and others in informal LIGO team discussions.

[12] L. D. Landau and E. M. Lifschitz, *Theory of Elasticity* (Pergamon Press, New York, 1986).

[13] At the moment there is no practical proposal to beat the Standard Quantum Limit which could be readily implemented in LIGO. However, conceptual schemes can be found in e.g.

A. V. Syrtsev and F. Ya. Khalili, JETP **79** (3), 409-413 (1994);

S. P. Vyatchanin and A. B. Matsko, Zh. Eksp. Teor. Fiz. v.110 (1996) 1253 (*English translation:* JETP v.83(4), 690 (1996));

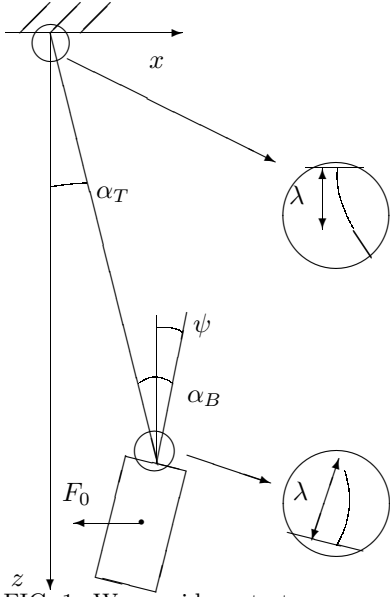V. B. Braginsky, M. L. Gorodetsky, F. Ya. Khalili, Physical Letters A **A232**, 340-348 (1997)

and references therein.

FIG. 1. We consider a test mass suspended on a single fiber. The fiber's bottom is attached to the top of the test mass, and the fiber's top is attached to the last stage of the seismic isolation stack. It is assumed that at attachment points the fiber is perpendicular to the surface to which it is attached.
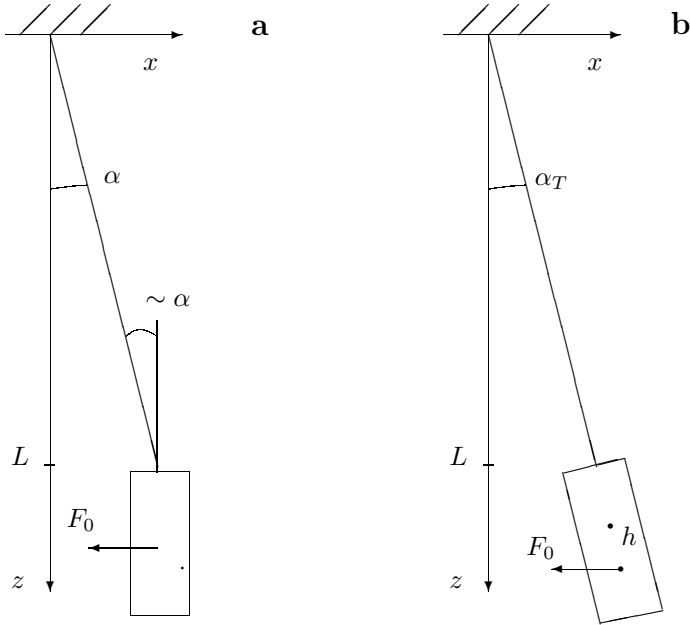

FIG. 2. Motion of the test mass and the suspension fiber under the action of an oscillating force applied at the center of the laser beam spot in two different cases: *a)* the beam spot is positioned at the mirror center, the fiber bends equally at the top and the bottom, and *b)* the position of the beam spot is shifted down from the center of the mirror, so that there is no bending of the fiber at the bottom.

13

FIG. 3. Fig. 3. A plot of $S_{\text{bottom}}(f)/S_{\text{top}}(f)$ as a function of frequency f for three different positions of the laser beam spot.
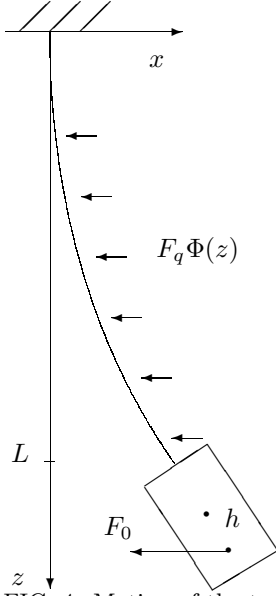

FIG. 4. Motion of the test mass and suspension fiber under the action of the generalized force F_q defined in Eq. (20) of the text. The force F_q should be chosen so that there is no bending of the fiber at it's top and bottom attachment points.
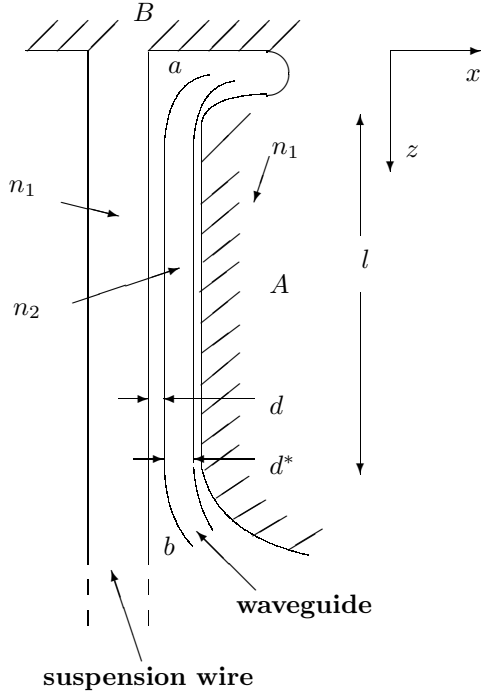

FIG. 5. A proposed scheme for compensation of a suspension thermal noise. The optical waveguide ab is positioned close to the suspension fiber made of fused silica. A horizontal displacement of the suspension fiber is recorded through a phase shift of an optical wave propagating through the waveguide.

Fig. 3